



Thermodynamic modeling of fcc order/disorder transformations in the Co–Pt system

DongEung Kim^{a,*}, James E. Saal^a, Liangcai Zhou^b, ShunLi Shang^a, Yong Du^b, Zi-Kui Liu^a

^a The Pennsylvania State University 304 Steidle Bldg., University Park, PA 16802, USA

^b State Key Laboratory of Powder Metallurgy, Central South University, Hunan, 410083, China

ARTICLE INFO

Article history:

Received 19 January 2011

Received in revised form

1 April 2011

Accepted 14 April 2011

Available online 12 May 2011

Keywords:

CALPHAD

Thermodynamic modeling

Co–Pt system

Order/disorder transformation

ABSTRACT

The present work reports on a thermodynamic modeling of the Co–Pt system with ordered fcc phases of L1₀ and L1₂ structures by means of the CALPHAD method. The liquid, hcp and fcc phases have been modeled as substitutional solutions where the interaction parameters are composition dependent in the form of the Redlich–Kister polynomial. The disordered and ordered fcc phases have been modeled in terms of the compound energy formalism with a single Gibbs energy function. The obtained phase equilibria and activities of Co and Pt agree well with the available experimental data. First-principles calculations are performed to obtain the enthalpies of formation for the ordered fcc phases at 0 K. These calculated enthalpies of formations for the ordered phases are less negative than the enthalpies of the disordered state at low temperatures determined from the CALPHAD modeling. The Fe–Pt and Ni–Pt systems exhibit the same feature as that in the Co–Pt system, which is discussed in terms of the total magnetic moment of ordered fcc phases.

© 2011 Elsevier Ltd. All rights reserved.

1. Introduction

Cobalt–platinum compounds have been used for their extraordinary catalysis properties in chemical reactions [1–3]. The L1₀ CoPt alloy has been studied for the development of ultrahigh density magnetic storage media [4,5]. The cobalt–platinum system is also an important component of the nickel based superalloy database such as in TTNi8 [6].

The cobalt–platinum system exhibits an order/disorder transformation in the fcc solid solution, where the disordered (A1) phase at high temperatures orders into the L1₀ structure near 50 at.% Pt and the L1₂ structure near 25 and 75 at.% Pt. This phenomenon is found in many binary systems between platinum and transition metals such as Ni and Fe [7,8]. A method for describing such fcc order/disorder transformations within the CALPHAD approach and the compound energy formalism has been developed using a four sublattice model [9]. The four sublattice model, as the name implies, uses four sublattices to describe the four sites in the fcc tetrahedron, distinguishing the A1, L1₂, and L1₀ structures. With this method, experimental thermodynamic data for the disordered state such as the enthalpy of mixing and those for the ordered states such as enthalpies of formation and enthalpies for the disordered to ordered phase transformation can be used to evaluate the model parameters.

Integrating first-principles predictions for the thermodynamics of phases into the CALPHAD approach has been proven to be very useful in investigating systems with limited experimental data [10]. However, using a combined first-principles/CALPHAD approach in the four sublattice model for the Ni–Pt system [8] has been shown to be problematic. In particular, the enthalpies of formation predicted by first-principles for the L1₂ and L1₀ structures are less negative than the enthalpies of the disordered state at low temperatures determined from the CALPHAD modeling for the Ni–Pt system [8].

In this paper, the fcc order/disorder transformation in the Co–Pt system is modeled using the CALPHAD approach and the four sublattice model. Experimental phase equilibria and thermochemical data are used to evaluate the model parameters. First-principles calculations for the enthalpies of formation of the ordered Co–Pt compounds, Co₃Pt, CoPt, and CoPt₃, are performed and shown to have similar issues with those found in the Ni–Pt system. The first-principles results of both the Ni–Pt and Co–Pt systems are compared with the corresponding CALPHAD modeling, where it is shown that the metastability of the ordered compounds increases with their total magnetic moments. The enthalpies of formation of the Fe–Pt ordered compounds are also calculated and shown to have the same issue.

2. Co–Pt literature review

The cobalt–platinum system contains an fcc solid solution from pure cobalt to pure platinum, with an order/disorder

* Corresponding author.

E-mail address: duk157@psu.edu (D.E. Kim).

transformation. An hcp solid solution is also present at cobalt-rich compositions. The activity of cobalt in liquid platinum was measured at 1850 K using the Knudsen effusion method by Alcock and Kubik [11]. The liquidus and solidus form a narrow two-phase region which was examined at Co-rich compositions by Gebhardt and Koster [12] and Nemilow and Anorg [13]. The enthalpy of mixing of the disordered fcc phase has been reviewed by Cyr et al. [14]. The enthalpies of formation for the L1₀ and CoPt₃ L1₂ phases were measured by Oriani and Murphy [15] at 914 K. Barmak et al. measured the enthalpies of transformation from disordered phase to L1₀ for CoPt thin films [16]. The fcc Curie temperature has been reported by several studies [12,17–20], showing its decrease with Pt content with a slightly positive deviation from linearity. Phase equilibrium data for hcp to fcc transformation has been reviewed by Zhao [21], where it was theorized that large scatter in the data is due to metastable martensitic transformations. Zhao analyzed the cooling and heating transformation-start temperature based on the fcc/hcp phase boundary assessed from the electron probe microanalysis (EPMA) results and found that all the cooling data are below the obtained fcc/(fcc + hcp) transus from EPMA results. Zhao concluded, therefore, when only cooling and heating data are available for a system such as Co–Pt system, the highest cooling data can be considered the most accurate data since the fcc/(fcc + hcp) phase boundary should be above all cooling data. From this consideration, the data of Newkirk et al. [22] was found the most reliable, although new experiments were recommended. Order/disorder transformations for the L1₀ and L1₂ phases have been reported by Leroux et al. [19], Newkirk et al. [22,23], and Gebhardt and Koster [12]. The long-range order (LRO) parameter for L1₀ was crystallographically determined from the lattice parameters by Rudman and Averbach [24]. Only one experimental report about the stability of Co₃Pt L1₂ by Inden [25] was found in the literature. The short-range order (SRO) parameters for Co₃Pt, Co₆₅Pt₃₅ and CoPt₃ alloys were experimentally determined from diffuse intensity measurement by Capitan et al. [26] and Kentzinger et al. [27], respectively.

The system has been previously modeled using the CALPHAD approach by Oikawa et al. [28], with a focus on the disordered fcc phase and its melting behavior, but the hcp phase and order/disorder transformation were not considered.

3. First-principles calculations

First-principles calculations based on density functional theory are performed with the Vienna *Ab initio* Simulation Package (VASP) [29,30]. Calculations are performed on the L1₀ and L1₂ ordered fcc structures for the Co–Pt, Fe–Pt and Ni–Pt systems. Pseudopotentials with the projector augmented wave method (PAW) [31] are employed and the exchange and correlation energy is determined with the generalized gradient approximation method of Perdew–Burke–Ernzerhof (PBE) [32] with an constant energy cutoff of 350 eV. The atomic arrangements are relaxed using the Methfessel–Paxton method [33] and at least 5000 *k*-points per reciprocal atom based on the Monkhorst–Pack scheme [34] for the Brillouin-zone sampling is used. All degrees of freedom are fully relaxed and the total energies and volumes are converged to within less than 1 meV and 0.1 Å³ per atom, respectively. All calculations are carried out with spin polarized.

The calculated total energies and lattice parameters of pure elements Co, Fe, Ni and Pt in fcc phase are listed in Table 1, showing good agreements with those calculated by Wang et al. [35] and the experimental lattice parameters [36]. Enthalpies of formation for the ordered phases with respect to the pure elements in the fcc structure are determined by the following equation:

$$\Delta_f H_{ord} = E_{ord} - x_X E_{FCC}^X - x_{Pt} E_{FCC}^{Pt} \quad (1)$$

where $\Delta_f H_{ord}$ is the enthalpy formation for the ordered phase (either L1₀ or L1₂), E_{ord} is the total energy of the ordered phase,

Table 1
Calculated total energies (E) and lattice parameters for fcc Co, Fe, Ni and Pt.

Pure elements (fcc structure)	E (eV/atom)	a (Å)	Reference
Co	–7.0916	3.501	This work
	–6.9696	3.518	[35]
	–	3.545	[36]
Fe	–8.1522	3.448	This work
	–8.1872	3.446	[35]
	–	3.647	[36]
Ni	–5.5708	3.498	This work
	–5.3902	3.517	[35]
	–	3.523	[36]
Pt	–6.0537	3.964	This work
	–6.0451	3.985	[35]
	–	3.923	[36]

E_{FCC}^X and E_{FCC}^{Pt} are the total energies of the element X (Co, Fe and Ni) and Pt in the fcc structure, respectively, and x_X and x_{Pt} are the mole fractions of elements X and Pt, respectively. The calculated lattice parameters, enthalpies of formation, and total magnetic moments are given in Tables 2–4 for the Co–Pt, Fe–Pt, and Ni–Pt ordered L1₀ and L1₂ compounds, respectively. The difference in the crystallographic parameters between first-principles and experiment is less than 1% for all compounds. The enthalpies of formation and total magnetic moments are in good agreement with other calculations and experimental data in the literature.

4. Thermodynamic modeling

The Gibbs energy descriptions for hcp, fcc, and liquid phases of pure Co and pure Pt are taken from the SGTE PURE element database [37]. The liquid, hcp, and fcc phases are described as substitutional solutions. The molar Gibbs energy for the disordered solution, G_m^{dis} , is defined by:

$$G_m = x_{Co} G_{Co}^0 + x_{Pt} G_{Pt}^0 + RT (x_{Co} \ln x_{Co} + x_{Pt} \ln x_{Pt}) + {}^E G_m + {}^{mag} G_m \quad (2)$$

where x_{Co} and x_{Pt} are the mole fractions of Co and Pt, respectively, G_{Co}^0 and G_{Pt}^0 are the Gibbs energies of pure Co and Pt in the phase of interest, and R is the gas constant. The excess Gibbs energy, ${}^E G_m$, is defined with the Redlich–Kister polynomial [38]:

$${}^E G_m = x_{Co} x_{Pt} \sum_{i=0}^n {}^i L (x_{Co} - x_{Pt})^i \quad (3)$$

where ${}^i L$ is the i th order interaction parameter between Co and Pt in the solution phase. The term ${}^{mag} G_m$ is a magnetic contribution to the Gibbs energy, expressed by the following equation [39]:

$${}^{mag} G_m = RT \ln (\beta + 1) f(\tau) \quad (4)$$

where β is the average magnetic moment and the function $f(\tau)$ is

$$f(\tau) = 1 - \frac{1}{A} \left[\frac{79\tau^{-1}}{140p} + \frac{474}{497} \left(\frac{1}{p} - 1 \right) \left(\frac{\tau^3}{6} + \frac{\tau^9}{135} + \frac{\tau^{15}}{600} \right) \right] \quad \tau < 1$$

$$f(\tau) = -\frac{1}{A} \left(\frac{\tau^{-5}}{10} + \frac{\tau^{-15}}{315} + \frac{\tau^{-25}}{1500} \right) \quad \tau \geq 1 \quad (5)$$

with

$$A = \frac{518}{1125} + \frac{11692}{15975} \left(\frac{1}{p} - 1 \right) \quad (6)$$

where p is the ratio of the long-range order and short-range order contributions which depends on the structure and was introduced as an empirical constant with the value of 0.28 for fcc Co and Ni and 0.4 for bcc Fe by Inden [40]. τ is defined as $\tau = T/T_C$ where T_C is the Curie temperature.

Table 2

Summary of first-principles results and experimental data for the ordered Co–Pt compounds. The reference states for the enthalpies of formation and mixing are the pure elements in the fcc structure.

	Co ₃ Pt	CoPt	CoPt ₃	Reference
<i>a</i> (Å)	3.654	3.809	3.885	FP (This work)
	3.664 [26]	3.811 [19]	3.857 [56]	Exp
	–	3.806 [56]	–	Exp
<i>c</i> (Å)	–	3.708	–	FP (This work)
	–	3.694 [19]	–	Exp
	–	3.684 [56]	–	Exp
μ_B /atom	1.402	1.131	0.736	FP (This work)
	1.455 [57]	1.15 [57]	0.735 [57]	Other calculations
	–	–	0.7 [58]	Exp
	–	–	0.618 [58]	Exp
	–	–	0.69 [60]	Exp
	–	1.06 [59]	0.68 [61]	Exp
	–	1.08 [59]	0.61 [62]	Exp
ΔH_f (kJ/mol-atom)	–6.635	–9.550	–6.494	FP (This work)
	–	–12.265	–11.205	CALPHAD at 914 K (This work)
	–	–13.6 ± 0.7 [15]	–12.8 ± 1.63 [15]	Exp (at 914 K)
ΔH_{mix} at 300 K (kJ/mol-atom)	–8.651	–11.229	–8.039	CALPHAD (This work)
Difference ($\Delta H_f - \Delta H_{mix}$) (kJ/mol-atom)	2.016	1.679	1.545	ΔH_f (0 K FP) – ΔH_{mix} (300 K) (This work)
	–	–3.1 ± 0.2	–	Exp at 783 K [16]
	–	–3.303	–	From present modeling at 783 K

Table 3

Summary of first-principles results and experimental data for the ordered Fe–Pt compounds. The reference states for the enthalpies of formation and mixing are the pure elements in the fcc structure.

	Fe ₃ Pt	FePt	FePt ₃	Reference
<i>a</i> (Å)	3.737	3.855	3.911	FP (This work)
	3.730 [19]	3.861 [56]	–	Exp
<i>c</i> (Å)	–	3.757	–	FP (This work)
	–	3.788 [56]	–	Exp
μ_B /atom	2.118	1.640	1.094	FP (This work)
	2.14	1.69	1.235	Other calculations [63]
	2.16 [64]	1.64 [65]	0.883 [66]	Exp
ΔH_f (kJ/mol-atom)	–19.361	–30.924	–23.233	FP (This work)
ΔH_{mix} at 300 K (kJ/mol-atom)	–44.250	–65.250	–48.938	CALPHAD [7]
Difference ($\Delta H_f - \Delta H_{mix}$) (kJ/mol-atom)	24.889	34.326	25.704	ΔH_f (0 K FP) – ΔH_{mix} (300 K) (This work)
	–	–10.2 ± 2.1	–	Exp at 673 K [16]
	–	–8.748	–	From CALPHAD [7] at 673 K

The four sublattice model is employed to describe the fcc phase, which is disordered A1 structure at high temperatures and becomes ordered in the L1₀ and L1₂ structures at lower temperatures. The four sublattice description represents the four atoms that form a tetrahedron in the fcc primitive cell. For the Co–Pt system, the sublattice model is (Co, Pt)_{0.25}(Co, Pt)_{0.25}(Co, Pt)_{0.25}(Co, Pt)_{0.25} in per mole of atoms and can reproduce the ordered fcc Pt compositions at 25%, 50%, and 75% with the end-members (Co)(Co)(Co)(Pt), (Co)(Co)(Pt)(Pt), (Co)(Pt)(Pt)(Pt), respectively. The Gibbs free energy for the fcc phase, G_m^{fcc} , is given by:

$$G_m = G_m^{\text{dis}}(x_i) + \Delta G_m^{\text{ord}}(y_i^s) \quad (7)$$

where $G_m^{\text{dis}}(x_i)$ is the molar Gibbs energy of the disordered fcc phase, and $\Delta G_m^{\text{ord}}(y_i^s)$ the molar ordering energy with y_i^s being the mole fraction of element i in sublattice s , often referred to as site fraction, and x_i the mole fraction of element i . The ordering energy, being zero when the phase is disordered, is expressed as:

$$\Delta G_m^{\text{ord}} = G_m^{\text{Asl}}(y_i^s) - G_m^{\text{Asl}}(y_i^s = x_i). \quad (8)$$

The Gibbs energy expression of the four sublattice compound energy formalism [9] is

$$G_m^{\text{Asl}}(y_i^s) = \sum_i \sum_j \sum_k \sum_l y_i^{(1)} y_j^{(2)} y_k^{(3)} y_l^{(4)} G_{ijkl}^0 + 0.25RT \sum_{s=1}^4 \sum_i y_i^{(s)} \ln(y_i^{(s)}) + E G_m^{\text{ord}} \quad (9)$$

where the first term describes the mechanical mixing of all the stoichiometric compounds, i.e. end-members, defined by the model, with G_{ijkl}^0 being the Gibbs energy of an end-member compound $ijkl$; the second term is the random mixing in each sublattice, and the last term is the excess term $E G_m^{\text{ord}}$ shown as follows:

$$E G_m^{\text{ord}} = \sum_{i_1} \sum_{i_2 > i_1} \sum_j \sum_k \sum_l y_{i_1}^{(1)} y_{i_2}^{(1)} y_j^{(2)} y_k^{(3)} y_l^{(4)} L_{i_1, i_2, j, k, l} + \dots + \sum_{i_1} \sum_{i_2 > i_1} \sum_{j_1} \sum_{j_2 > j_1} \sum_k \sum_l y_{i_1}^{(1)} y_{i_2}^{(1)} y_{j_1}^{(2)} y_{j_2}^{(2)} y_k^{(3)} y_l^{(4)} \times L_{i_1, i_2, j_1, j_2, k, l} + \dots \quad (10)$$

Table 4
Summary of first-principles results and experimental data for the ordered Ni–Pt compounds. The reference states for the enthalpies of formation and mixing are the pure elements in the fcc structure.

	Ni ₃ Pt	NiPt	NiPt ₃	Reference
<i>a</i> (Å)	3.659 –	3.844 3.873 [67]	3.880 –	FP (This work) Exp
<i>c</i> (Å)	– –	3.625 3.589 [67]	– –	FP (This work) Exp
μ_B /atom	0.606 0.50–0.62 [68] 0.43 [70]	0.525 0.51 [69] 0.2 [70]	0.279 0.28 [69] 0 [70]	FP (This work) FP (Other calculations) Exp
ΔH_f (kJ/mol-atom)	–7.383 –8.27 –8.75 –6.57 – –	–9.701 –11.42 –11.76 –7.64 –8.98 –9.27	–6.790 –8.4 –11.98 –6.31 – –	FP (This work) FLMTO + CWM [71] LMTO + CPA [72] VASP (no relaxation) [8] VASP (relaxation) [8] Exp (at 298.15 K) [73]
ΔH_{mix} at 300 K (kJ/mol-atom)	–7.643	–9.343	–5.814	CALPHAD [8]
Difference ($\Delta H_f - \Delta H_{mix}$) (kJ/mol-atom)	–0.097	–1.032	–1.427	ΔH_f (0 K FP) – ΔH_{mix} (300 K) (This work)

In the above equation, comma separates interacting constituents in the same sublattice, and column separates the sublattices. The first summation describes the interaction parameters in one sublattice, $L_{i_1, i_2; j; k; l}$, which represents interactions between i_1 and i_2 in the first sublattice when the other three sublattices are occupied by constituents j , k and l , respectively. The same applies to interactions in the second, third, and fourth sublattices. The second summation is related to the reciprocal parameters which describe simultaneous interactions of i_1 and i_2 in the first sublattice and j_1 and j_2 in the second sublattice, while the other two sublattices (3rd and 4th) are occupied by constituents k and l , respectively. These are the parameters that describe the contribution to the Gibbs energy due to the short-range ordering as presented by Sundman et al. [9]. The number of possible interaction parameters is very large, but many have very similar values due to the symmetry in Gibbs energy function.

5. Results and discussion

The PARROT module of Thermo-Calc [41] is employed to evaluate the model parameters in Gibbs energy function from the experimental thermochemical and phase equilibria data. The activity data of Alcock and Kubik [11] in liquid and Hultgren [42] in fcc, the solidus data of Gebhardt and Koster [12] and Nemilow and Anorg [13], the Curie temperature of the fcc phase [12,17–20], and the thermodynamic data of Cyr et al. [14] are used to evaluate the interaction parameters in the fcc phase. The calculated results are compared with the experimental data from Figs. 1 to 5, respectively, showing that all experimental data are well reproduced by the current model parameters. It should be mentioned that the model parameters for the disordered fcc and liquid phases are nearly identical to those determined by Oikawa et al. [28] as the same datasets were used to evaluate these interaction parameters for these phases. The composition dependence of the Curie temperature in hcp is assumed to be the same as that in fcc due to the lack of experimental data.

The fcc/hcp phase equilibria data of Newkirk et al. [22] is used to determine the parameters and the calculated phase boundaries are shown in Fig. 6. As we mentioned in Section 2, the experimental data are somewhat scattered due to metastable martensitic transformation. The open symbols represent the transformation starting temperatures on heating and the closed symbols the transformation starting temperatures on cooling. It should be noted that the CALPHAD predicted fcc/(fcc + hcp) phase

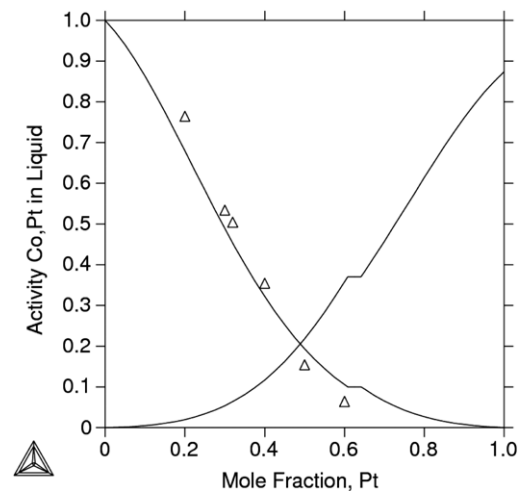


Fig. 1. Activity of Co and Pt in the liquid phase at 1850 K with experimental data [11]. The reference states for Co and Pt are the pure elements in liquid.

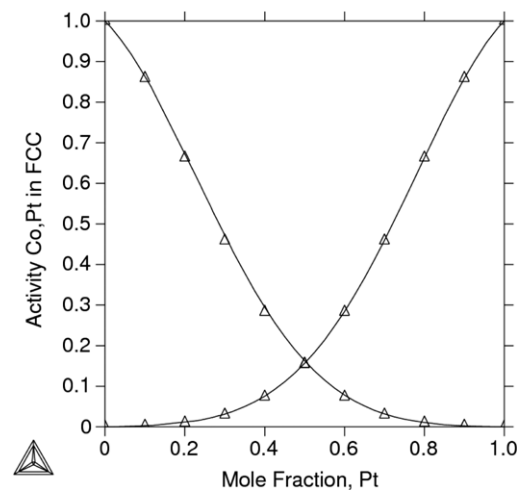


Fig. 2. Activity of Co and Pt in the fcc phase at 1273 K with experimental data [42]. The reference states for Co and Pt are the pure elements in fcc.

boundary is above all cooling data. The experimental data between 650–750 K on cooling were considered to be the martensitic

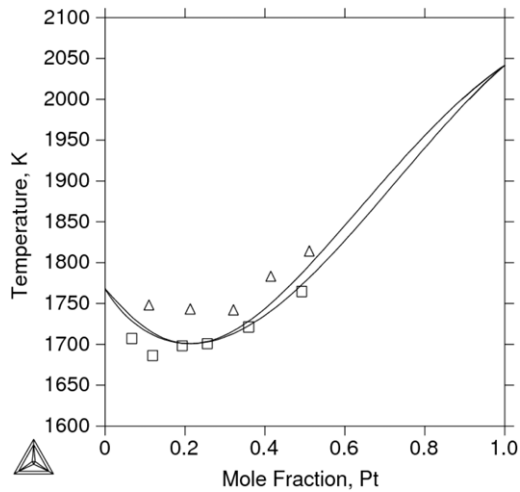


Fig. 3. Calculated liquidus and solidus of the Co-Pt phase diagram with experimental data (squares [12], triangles [13]).

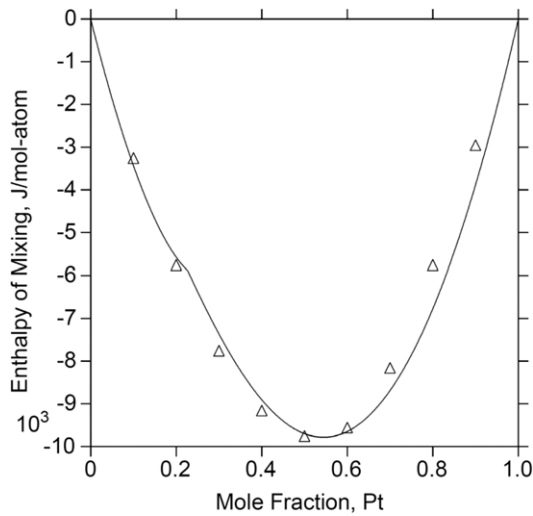


Fig. 4. Enthalpy of mixing in fcc phase at 1173 K with reviewed data [14].

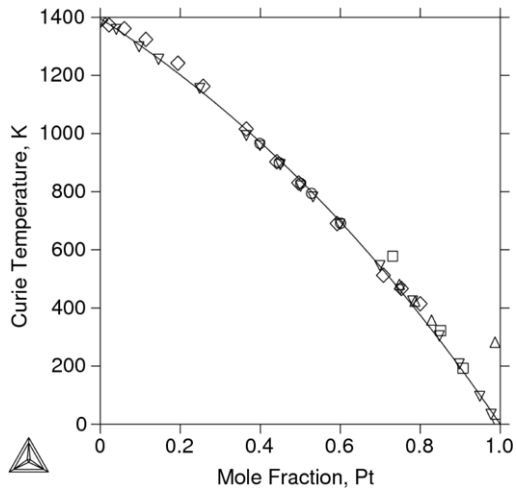


Fig. 5. Calculated Curie temperature of the fcc phase with experimental data (diamonds [12], squares [17], triangles [18], circles [19], reverse triangles [20]).

transformation-start temperature in Zhao's analysis [21], which are not used in the present modeling.

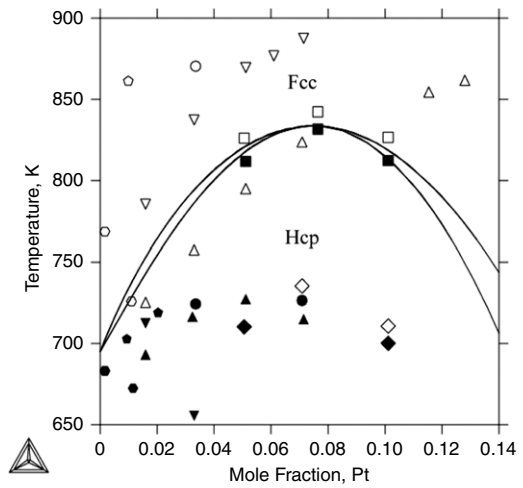


Fig. 6. Hcp/fcc phase equilibria and experiments. (circles [74], triangles [75], squares [22], diamonds [23], reverse triangles [76], pentagon [77], hexagon [78]) Closed symbols represent the cooling transformation-start temperature and open symbols the heating transformation-start temperatures.

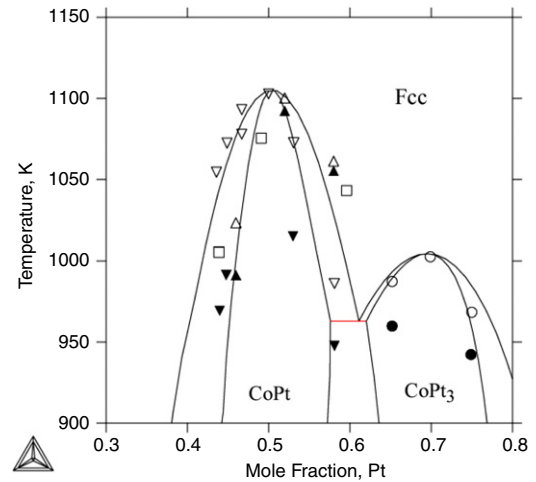


Fig. 7. Fcc order/disorder temperatures with experiments. (triangles [22,23], squares [12], reverse triangles and circles [19]) Open symbols - disorder/disorder + order phase boundary, closed symbols - disorder + order/order phase boundary.

The order/disorder transformation temperatures for L1₀ and L1₂ from Leroux et al. [19], Newkirk et al. [22,23], and Gebhardt and Koster [12] are used to determine $\Delta_f H_{ord}$ and $\Delta_f S_{ord}$ for ordered Co₃Pt, CoPt, and CoPt₃, and the interaction parameters. The resulting phase equilibria are shown in Fig. 7. The complete phase diagram for the Co-Pt system from the present CALPHAD modeling is shown in Fig. 8 with the superimposed experimental data. Co₃Pt is predicted to be stable up to about 822 K. This behavior is similar to that measured by Inden [25] with a congruent temperature of approximately 840 K. The calculated enthalpies of formation of CoPt and CoPt₃ at 914 K from the CALPHAD modeling are compared with the available measurements [15] in Table 2, showing a good agreement. The calculated enthalpy for the disordered fcc phase to L1₀ transformation in CoPt compound at 783 K from the current modeling is -3.303 kJ/mol-atom which is also in a good agreement with the experimental data (-3.1 ± 0.2 kJ/mol-atom) in the literature [16].

The Bragg-Williams LRO parameter, η [43–45], is expressed by

$$\eta = \frac{p_A^{(a)} - c_A}{1 - \nu} \quad (11)$$

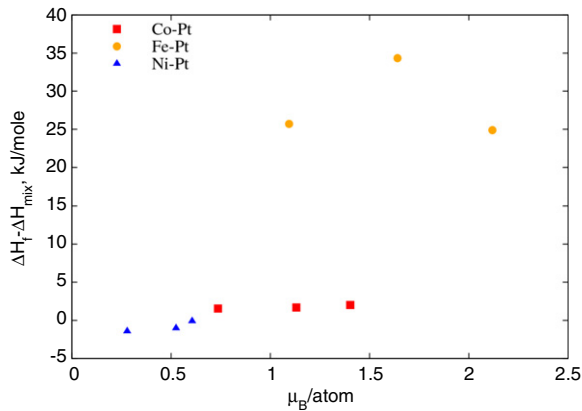


Fig. 11. Difference between the first-principles predicted enthalpies of formation of the ordered fcc compounds and the CALPHAD predicted enthalpies of mixing of the disordered fcc phase at 300 K versus the calculated total atomic magnetic moment of the ordered compounds.

Table 5
CALPHAD thermodynamic modeling parameters for the phases in the Co–Pt system, in J/mol-atom.

Phase	Evaluated parameters
Liquid	${}^0L_{\text{Co,Pt}}^{\text{liq}} = -54724$
	${}^1L_{\text{Co,Pt}}^{\text{liq}} = -3619$
hcp	${}^0L_{\text{Co,Pt}}^{\text{hcp}} = -48399$
	${}^1L_{\text{Co,Pt}}^{\text{hcp}} = -6149$
	${}^0T_{\text{Co,Pt}}^{\text{hcp}} = 565$
	${}^1T_{\text{Co,Pt}}^{\text{hcp}} = -59$
fcc-A1(disordered part of fcc)	${}^0L_{\text{Co,Pt}}^{\text{fcc}} = -49694$
	${}^0T_{\text{Co,Pt}}^{\text{fcc}} = 565$
	${}^1T_{\text{Co,Pt}}^{\text{fcc}} = -59$
Ordered fcc	$G_{\text{Co:Co:Co:Pt}} = \dots = G_{\text{Pt:Co:Co:Co}} = -18344 - 1.575 \times T$
	$G_{\text{Co:Co:Pt:Pt}} = \dots = G_{\text{Pt:Pt:Co:Co}} = -25678 - 2.586 \times T$
	$G_{\text{Pt:Pt:Pt:Co}} = \dots = G_{\text{Co:Pt:Pt:Pt}} = -21867 + 1.020 \times T$
	${}^0L_{\text{Co,Pt:Co,Pt:Co}} = -6394 + 1.873 \times T$

In the case of the Cu–Pt system [47], which is a non-magnetic system having a continuous fcc solid solution phase and ordered phases at low temperature, the first-principles calculated enthalpies of formation for the stable $L1_0/L1_2$ compounds are more negative than the CALPHAD predicted enthalpies of mixing for the disordered fcc phase, as expected. We also calculated the enthalpies of formation of $L1_2\text{-AlPt}_3$ and $L1_2\text{-InPt}_3$, which are stable ordered fcc phases in Al–Pt [48] and In–Pt [49] systems, respectively, and compared with the CALPHAD predicted enthalpies of mixing for the disordered fcc phase. It is also found that the first-principles calculated enthalpies of formation of those compounds are more negative than the CALPHAD predicted enthalpies of mixing from the Al–Pt and In–Pt systems, respectively, as expected. This supports the argument that the disagreement between first-principles and CALPHAD for Co–Pt, Fe–Pt, and Ni–Pt systems are related the magnetic properties of the system.

In the present work, the vibrational contribution is not considered for ordered compounds since it is expected to be negligible. van de Walle et al. [50] studied the vibrational entropy of ordered and disordered Ni_3Al through the first-principles calculations and they found a remarkably small value of vibrational entropy difference between ordered and disordered Ni_3Al , which is around 0.05 kB/atom. Recently, Shang et al. [51] also studied the vibrational properties of ordered and disordered $\text{Ni}_{1-x}\text{Pt}_x$ alloys from first-principles calculations and they showed that the

vibrational entropy difference between ordered and disordered NiPt is around 0.13 kB/atom from 200 to 1000 K, which corresponds about 300 J/mol-atom at 300 K. This difference also agrees well with the value between the ordered and disordered CuAu [52] and its contribution is even smaller in the case of $L1_2$ phase. Shang et al. [51] pointed out that the configurational entropy is more important than the vibrational entropy. Thus, we assume that the vibrational contribution for Co–Pt system is also small and it does not significantly affect the calculated phase stability between ordered and disordered phases in the present work because enthalpy differences between ordered and disordered phases for the Co–Pt system is on the order of kJ/mol-atom.

For the Fe–Pt system the energy difference is larger by an order of magnitude than that in the Co–Pt system. It should be noted that the thermodynamic modeling of the Fe–Pt system employed no experimental enthalpies of mixing for the disordered fcc phase [7], whereas such data were used in the Co–Pt and previous Ni–Pt modeling. Although a larger enthalpy difference is expected due to the higher magnetic moment in the Fe–Pt compounds, the large jump in the difference suggests that the CALPHAD prediction of the enthalpy of mixing in Fe–Pt may be inaccurate, which was noted by Fredriksson and Sundman [7]. Nevertheless, further investigations are needed to bridge the gap between first-principles calculations and CALPHAD modeling for magnetic phases. The recent works in our group [53–55] may point to the right direction to pursue.

The thermodynamic parameters for the Co–Pt system obtained in the present work are listed in Table 5.

6. Summary

In the present work, a thermodynamic description of the Co–Pt system, which has an order/disorder transformation in the fcc solid solution, is obtained using the CALPHAD approach. The ordered fcc phases are modeled by using a four sublattice model. The calculated phase diagram and thermodynamic properties agree well with the available experimental data in the literature. The temperature dependence of long-range order parameter for $L1_0$ structure and the composition dependence of the short-range order parameter in the disordered fcc phase are calculated and compared with available experimental data. The first-principles calculations are performed to obtain the enthalpies of formation for the ordered fcc phases at 0 K in order to assist the thermodynamic modeling but those results are not used in the modeling since they are less negative than the enthalpies of the disordered state at low temperatures determined from the CALPHAD modeling. The Fe–Pt and Ni–Pt systems also show the same feature at that in the Co–Pt system. The energy difference between the CALPHAD predicted enthalpy of mixing of the disordered fcc phase and the first-principles predicted enthalpies of formation for the $L1_0$ and $L1_2$ structures for the Co–Pt, Fe–Pt, and Ni–Pt systems increase as increasing the total magnetic moment of their ordered fcc compounds. It suggests that this disagreement between first-principles and CALPHAD is partially due to the magnetic properties of the system.

Acknowledgments

This work is funded by the Office of Naval Research (ONR) under the contract number N0014-07-1-0638. We thank the program manager Dr. David Shifler for his support and encouragement. The financial supporting from National Natural Science Foundation of China (Grant No. 51028101) is also acknowledged. First-principles calculations were carried out on the LION clusters at the Pennsylvania State University supported by the Materials Simulation Center and the Research Computing and Cyberinfrastructure unit at the Pennsylvania State University. Calculations were also carried

out on the INTI clusters from the computer science department at Pennsylvania State University supported by NSF under Grant No. CISE-0202007 and CyberStar cluster funded by NSF through grant OCI-0821527.

Appendix. Supplementary data

Supplementary material related to this article can be found online at doi:10.1016/j.calphad.2011.04.005.

References

- [1] X.M. Wang, N. Li, L.D. Pfefferle, G.L. Haller, *J. Phys. Chem. C* 114 (40) (2010) 16996–17002.
- [2] S.E. Maisuls, K. Seshan, S. Feast, J.A. Lercher, *Appl. Catal. B-Environ.* 29 (1) (2001) 69–81.
- [3] L.B. Gutierrez, A.V. Boix, E.A. Lombardo, J.L.G. Fierro, *J. Catal.* 199 (1) (2001) 60–72.
- [4] D. Weller, A. Moser, L. Folks, M.E. Best, W. Lee, et al., *IEEE Trans. Magn.* 36 (1) (2000) 10–15.
- [5] D.J. Sellmyer, M. Yu, R.A. Thomas, Y. Liu, R.D. Kirby, *Phys. Low-Dimens. Struct.* 1–2 (1998) 155–165.
- [6] ThermoTECH Ni-based Superalloys Database, TTNi8, Version 8.0, Thermo-Calc Software AB, Stockholm, Sweden.
- [7] P. Fredriksson, B. Sundman, *CALPHAD* 25 (4) (2001) 535–548.
- [8] X.G. Lu, B. Sundman, J. Agren, *CALPHAD* 33 (3) (2009) 450–456.
- [9] B. Sundman, S.G. Fries, W.A. Oates, *CALPHAD* 22 (3) (1998) 335–354.
- [10] Z.K. Liu, *J. Phase Equilib. Diffus.* 30 (5) (2009) 517–534.
- [11] C.B. Alcock, A. Kubik, *Trans. Inst. Min. Met.* 77 (1968) 220–224.
- [12] V.E. Gebhardt, W. Koster, *Z. Met.kd.* 32 (1940) 253–261.
- [13] W.A. Nemilow, *Z. Anorg. Allg. Chem.* 213 (3) (1933) 283–291.
- [14] J.P. Cyr, J. Dellacherie, D. Balesdent, *J. Chem. Eng. Data* 26 (2) (1981) 174–178.
- [15] R. Oriani, W.K. Murphy, *Acta Metall.* 10 (SEP) (1962) 879–885.
- [16] K. Barmak, J. Kim, S. Shell, E.B. Svedberg, J.K. Howard, *Appl. Phys. Lett.* 80 (22) (2002) 4268–4270.
- [17] F.W. Constant, *Phys. Rev.* 36 (11) (1930) 1654–1660.
- [18] A.W. Simpson, R.H. Tredgold, *Proc. Phys. Soc. London. Secion B* 67 (409) (1954) 38–41.
- [19] C. Leroux, M.C. Cadeville, V. Pierronbohnès, G. Inden, F. Hinz, *J. Phys. F Met. Phys.* 18 (9) (1988) 2033–2051.
- [20] J.M. Sanchez, J.L. Moranlopez, C. Leroux, M.C. Cadeville, *J. Phys.: Condens. Matter.* 1 (2) (1989) 491–496.
- [21] J.C. Zhao, *Z. Metallk.* 90 (3) (1999) 223–232.
- [22] J.B. Newkirk, A.H. Geisler, D.L. Martin, R. Smoluchowski, *J. Met.* 2 (10) (1950) 1249–1260.
- [23] J.B. Newkirk, R. Smoluchowski, A.H. Geisler, D.L. Martin, *J. Appl. Phys.* 22 (3) (1951) 290–298.
- [24] P.S. Rudman, B.L. Averbach, *Acta Metall.* 5 (2) (1957) 65–73.
- [25] G. Inden, *Mater. Res. Soc. Symp. Proc.* 19 (1983) 175–188. (Alloy Phase Diagrams).
- [26] M.J. Capitan, S. Lefebvre, Y. Calvayrac, M. Bessiere, P. Cenedese, *J. Appl. Crystallogr.* 32 (1999) 1039–1049.
- [27] E. Kentzinger, V. Parasote, V. Pierron-Bohnès, J.F. Lami, M.C. Cadeville, et al., *Phys. Rev. B* 61 (22) (2000) 14975–14983.
- [28] K. Oikawa, G.W. Qin, T. Ikeshoji, O. Kitakami, Y. Shimada, et al., *J. Magn. Magn. Mater.* 236 (1–2) (2001) 220–233.
- [29] G. Kresse, J. Furthmuller, *Phys. Rev. B* 54 (16) (1996) 11169–11186.
- [30] G. Kresse, J. Furthmuller, *Comput. Mater. Sci.* 6 (1) (1996) 15–50.
- [31] G. Kresse, D. Joubert, *Phys. Rev. B* 59 (3) (1999) 1758–1775.
- [32] J.P. Perdew, K. Burke, M. Ernzerhof, *Phys. Rev. Lett.* 77 (18) (1996) 3865–3868.
- [33] M. Methfessel, A.T. Paxton, *Phys. Rev. B* 40 (6) (1989) 3616–3621.
- [34] H.J. Monkhorst, J.D. Pack, *Phys. Rev. B* 13 (12) (1976) 5188–5192.
- [35] Y. Wang, S. Curtarolo, C. Jiang, R. Arroyave, T. Wang, et al., *CALPHAD* 28 (1) (2004) 79–90.
- [36] P. Villars, *Pearson's Handbook of Crystallographic Data for Intermetallic Phases*, ASTM International, Newbury, OH, 1991.
- [37] A.T. Dinsdale, *CALPHAD* 15 (4) (1991) 317–425.
- [38] O. Redlich, A.T. Kister, *Ind. Eng. Chem.* 40 (2) (1948) 345–348.
- [39] M. Hillert, M. Jarl, *CALPHAD* 2 (3) (1978) 227–238.
- [40] G. Inden, *Physica B & C* 103 (1) (1981) 82–100.
- [41] B. Sundman, B. Jansson, J.O. Andersson, *CALPHAD* 9 (2) (1985) 153–190.
- [42] R.R. Hultgren, Selected values of the thermodynamic properties of the elements, American Society for Metals, Metals Park, Ohio, 1973.
- [43] W.L. Bragg, E.J. Williams, *Proc. R. Soc. Lond. A-Math. Phys. Sci.* 145 (1934) 699–730.
- [44] W.L. Bragg, E.J. Williams, *Proc. R. Soc. Lond. A-Math. Phys. Sci.* 151 (1935) 540–566.
- [45] W.L. Bragg, E.J. Williams, *Proc. R. Soc. Lond. A-Math. Phys. Sci.* 152 (1935) 231–252.
- [46] T. Abe, B. Sundman, *CALPHAD* 27 (4) (2003) 403–408.
- [47] T. Abe, B. Sundman, H. Onodera, *J. Phase Equilib. Diffus.* 27 (1) (2006) 5–13.
- [48] K.S. Wu, Z.P. Jin, *J. Phase Equilib.* 21 (3) (2000) 221–226.
- [49] Y. Liang, C.P. Guo, C.R. Li, Z.M. Du, *J. Alloys Compd.* 475 (1–2) (2009) 220–226.
- [50] A. van de Walle, G. Ceder, U.V. Waghmare, *Phys. Rev. Lett.* 80 (22) (1998) 4911–4914.
- [51] S.L. Shang, Y. Wang, D. Kim, C.L. Zacherl, Y. Du, et al., *Phys. Rev. B* 83 (14) (2011) 144204.
- [52] V. Ozolins, C. Wolverton, A. Zunger, *Phys. Rev. B* 58 (10) (1998) R5897–R5900.
- [53] Y. Wang, S.L. Shang, H. Zhang, L.Q. Chen, Z.K. Liu, *Phil. Mag. Lett.* 90 (12) (2010) 851–859.
- [54] S.L. Shang, Y. Wang, Z.K. Liu, *Phys. Rev. B* 82 (1) (2010) 014425.
- [55] S.L. Shang, Y. Wang, D. Kim, Z.K. Liu, *Comput. Mater. Sci.* 47 (4) (2010) 1040–1048.
- [56] I. Galanakis, M. Alouani, H. Dreysse, *Phys. Rev. B* 62 (10) (2000) 6475–6484.
- [57] S. Polesya, S. Mankovsky, O. Sipr, W. Meindl, C. Strunk, et al., *Phys. Rev. B* 82 (21) (2010) 214409.
- [58] R.J. Lange, S.J. Lee, D.W. Lynch, P.C. Canfield, B.N. Harmon, et al., *Phys. Rev. B* 58 (1) (1998) 351–358.
- [59] W. Grange, I. Galanakis, M. Alouani, M. Maret, J.P. Kappler, et al., *Phys. Rev. B* 62 (2) (2000) 1157–1166.
- [60] K. Iwashita, T. Oguchi, T. Jo, *Phys. Rev. B* 54 (2) (1996) 1159–1162.
- [61] E.T. Kulatov, Y.A. Uspenskii, S.V. Halilov, *J. Magn. Magn. Mater.* 163 (3) (1996) 331–338.
- [62] F. Menzinger, A. Paoletti, *Phys. Rev.* 143 (2) (1966) 365.
- [63] Y.S. Gu, J. He, X.Y. Zhan, Z. Ji, Y. Zhang, et al., *Mater. Sci. Forum* 475–479 (2005) 3103–3106.
- [64] J. Inoue, M. Shimizu, *J. Phys. F Met. Phys.* 13 (12) (1983) 2677–2684.
- [65] S. Akiyama, Y. Tsunoda, *J. Magn. Magn. Mater.* 310 (2) (2007) 1844–1846.
- [66] J. Honolka, T.Y. Lee, K. Kuhnke, A. Enders, R. Skomski, et al., *Phys. Rev. Lett.* 102 (6) (2009) 4.
- [67] U. Esch, A. Schneider, *Z. Elektrochem. Angew. Phys. Chem.* 50 (1944) 268–274.
- [68] S.L. Shang, Y. Wang, Y. Du, Z.K. Liu, *Intermetallics* 18 (5) (2010) 961–964.
- [69] X.L. Che, J.H. Li, Y. Dai, B.X. Liu, *Sci. China Ser. E-Technol. Sci.* 52 (9) (2009) 2681–2687.
- [70] R.E. Parra, J.W. Cable, *Phys. Rev. B* 21 (12) (1980) 5494–5504.
- [71] C. Amador, W.R.L. Lambrecht, M. Vanschilfgaarde, B. Segall, *Phys. Rev. B* 47 (22) (1993) 15276–15279.
- [72] A.V. Ruban, I.A. Abrikosov, H.L. Skriver, *Phys. Rev. B* 51 (19) (1995) 12958–12968.
- [73] R.A. Walker, J.B. Darby, *Acta Metall. Mater.* 18 (12) (1970) 1261–1266.
- [74] E. Gebhardt, W. Koster, *Z. Met.kd.* 32 (1940) 253–261.
- [75] W. Koster, *Z. Met.kd.* 40 (1949) 431–432.
- [76] E. Raub, *Rev. Met.* 52 (1955) 429–440.
- [77] A.S. Darling, *Platinum Met. Rev.* 7 (3) (1963) 96–104.
- [78] W. Krajewski, J. Krueger, H. Winterhager, *Cobalt (English Edition)* 47 (June), 81–8; 48 (Sept.) (1970) 120–128.